applied sciences

MDPI

Article

Effects of a Hydraulic Series Connection and Flow Direction on Electricity Generation in a Stack Connected with Different Volume MFCs

Jaecheul Yu

Department of Civil and Environmental Engineering, Pusan National University, Busan 46241, Korea; yjcall0715@pusan.ac.kr

Abstract: Three microbial fuel cells (MFCs) with different volumes (S-, M-, and L-MFCs) were operated at individual flow (phase I) and serially connected flow modes (phase II for forward flow and phase III for reverse flow) at the same flow rate. The three MFCs showed different voltages and power generation according to the hydraulic and electric connection modes. The M- and L-MFCs showed a similar voltage at hydraulic series-forward flow mode (phase II). The principal component analysis (PCA) and Pearson correlation showed that voltage generation and power density were affected by volume, hydraulic retention time (HRT), chemical oxygen demand (COD) loading rate, removed COD, and internal resistances. When they were connected electrically in series and parallel, the stack showed relatively lower voltage loss (28–30%) compared to the voltage losses of the other stacks (43–94%). These results suggest an easy way to connect MFCs with different volumes can be a new option to avoid voltage reversal and minimize energy loss.

Keywords: hydraulic connection; electric connection; series; parallel; stack; voltage loss

check for updates

Citation: Yu, J. Effects of a Hydraulic Series Connection and Flow Direction on Electricity Generation in a Stack Connected with Different Volume MFCs. *Appl. Sci.* **2021**, *11*, 1019. https://doi.org/10.3390/app11031019

Academic Editor: Dino Musmarra

Received: 22 December 2020

Accepted: 21 January 2021

Published: 23 January 2021

1. Introduction

Microbial fuel cells (MFCs) are considered a promising technology for electricity generation from the oxidation of organic/inorganic using bacteria [1,2]. Although the power generated by MFCs has increased 10,000-fold from 1999 to 2009 [3], recently a MFC using fermentation filtrate produced a maximum power density (MPD) of 160 W/m^3 [4]. A single MFC unit generally produces a voltage of ~0.5 V due to energy utilization by bacteria, electrode overpotential and high internal resistance [5]. Nevertheless, the power generated form a single MFC was too low to be used even in low consumption devices [6]. Many studies have been performed to improve the energy production of MFCs.

A stacked system is one possible way of overcoming the low power of a single MFC, and various studies on stacked systems have been performed. A stack of four bio-polar plate MFCs achieved a high MPD of 144 W/m^3, which is 13 times higher than that of a single MFC [7]. A membraneless and single-chamber MFC stack in series produced a higher MPD of 22.8 mW/m^2, which was 2.5 times higher than the non-stack MFC units [8].

On the other hand, voltage reversal can occur in a stacked system due to a voltage imbalance between MFC units caused by a lack of substrate in the anode compartment, which can decrease power production [9,10]. A potential drop occurs when MFC units sharing anolyte are connected in series [11]. A tubular air-cathode MFC stack system showed a 35% lower MPD (67.5 W/m^2) than individual MFC (105.1 mW/m^2). The actual MPD of the MFC stack consisting of 12 cassette electrodes (115 W/m^3) was approximately 40% lower than the estimated MPD (182 W/m^3) because of the power imbalance of the individual MFCs [12]. A single chamber MFC stack comprised of four MFC units produced 13–45% lower MPDs (14.3 W/m^3 for a series connection and 22.8 W/m^3 for a parallel connection) than an individual MFC (26.2 W/m^3) [13]. Individual MFCs showed different cell voltage and MPDs in a submerged-exchangeable MFC stack system consisting of six MFCs [14].

Several approaches have been used to prevent voltage imbalance and reversal, and many methods can be used to prevent voltage reversal. First, the active bypass method can stop voltage reversal by bypassing the excessive current and voltage from superior cells to inferior cells and equalizes the voltage in a stacked system [15]. A serially stacked MFC stack using the cell balance system maintains the cell voltage of individual MFCs [16,17]. On the other hand, this method is not suitable for small-scale MFCs and requires complicated systems such as voltage controllers, magnets, and switches [9,15]. Second, the passive bypass method using semiconductor diodes can equalize the voltage and control voltage reversal in a stacked system [15]. This method cannot prevent voltage reversal completely, and the energy loss of the diodes can be high [9]. Finally, the charged and discharged method can avoid voltage reversal and minimize the energy loss in a stack system [18]. An MFC stack using a capacitor produced a stable MPD regardless of the variable performance of individual MFCs [18]. On the other hand, this method also requires complicated systems, such as a capacitor, controller, and switches. Therefore, a novel and more straightforward method to overcome the voltage imbalance and voltage reversal needed for practical applications.

The electricity production of an MFC stack system is affected by the electric connection method (in series and parallel), hydraulic flow modes (in series and parallel), reactor configuration, and operating conditions [19]. In particular, the parallel electrode connection system in hydraulically series flow mode achieved the highest MPD of 420 mW/m^2 (12.8 W/m^3) [19]. Therefore, the hydraulic flow modes can be a significant issue for the practical applications of a stacked MFC system. The novel MFC stack consisted of four units operating in hydraulic parallel flow mode showed a uniform power generation for all individual MFCs [6]. However, in the case of hydraulic parallel flow mode considerable cost may arise due to the large number of inflow pumps for fuel supply. In contrast, in the case of hydraulic series flow mode, a voltage imbalance can occur because the chemical oxygen demand (COD) loading rate and COD removed are different according to the position of each MFC unit in an MFC stack.

The electricity generation of an MFC is also affected by the COD loading rate (CLR) and COD removed. In particular, an MFC using a pure culture was reported to show good linear relationships between power generation and CLR when using an identical influent source [20]. The coulombic efficiency and energy recovery are calculated from the COD removed, meaning that the amount of COD removed would affect the MFC performance. The hydraulic retention time (HRT) is an important factor affecting the CLR and COD removed, which can be controlled by the flow rate or reactor volume. In most cases, HRT is controlled by the flow rate. Nevertheless, it is difficult to control the HRT of each MFC in a hydraulic series-connected stack system through the flow rate. This is because an MFC with the same volume is typically used for the stack system, and the stack system has been operated at the same flow rate. The HRT of each MFC in the stack system consisting of MFCs of different volumes can be controlled. On the other hand, there are no reports the performance of MFC stack consisting of MFCs with different volumes.

Therefore, this study investigated the performance of an MFC stack system comprised of three MFCs with different volumes and operated according to the hydraulic connection and electric connection methods. The performance was evaluated in terms of the voltage production, power density, energy recovery, and COD removal efficiency. These results will provide a unique option for the practical MFC applications to wastewater treatment.

2. Materials and Methods

2.1. MFC Configurations

The MFC stack system consisted of three MFC units with different volumes (19.2 mL for S-MFC, 38.4 mL for M-MFC, and 76.8 mL for L-MFC) (Table 1), and each MFC had two separator electrode assemblies sharing an anode compartment (Figure 1) [21]. Graphite felt (GF-20-5F, Nippon Carbon Inc., Tokyo, Japan) was used as the anode. The air-cathodes were 30% wet-proof carbon cloth (E-Tek, BASF Fuel Cell, Inc., Florham Park, NJ, USA) with platinum (Pt) as the catalyst and polytetrafluoroethylene (PTFE, 10 wt.%) as the diffusion layer, were treated, as reported previously [22]. A polypropylene non-woven fabric (Korea Non-Woven Tech. Co, Ltd., Busan, Korea) was used as the separator [19]. The anode and cathode were connected with a copper wire with an external resistances (Rext) of 1 kΩ.

Table 1. Configuration of small (S-), medium (M-), and large (L-) microbial fuel cells (MFCs) used in a stack system.

MFC	Total Anode Size [1] (cm^2)	Inter-SEA Distance [2] (cm)	Volume (mL)	AVR [3] (m^2/m^3)
S-MFC	96	0.4	19.2	500
M-MFC	96	0.8	38.4	250
L-MFC	96	1.6	76.8	125

[1] The sum of each anode size in two SEAs. [2] The thickness of anode chamber. [3] The ratio of total anode area for volume (AVR = [total anode size (m^2)/reactor volume (m^3)].

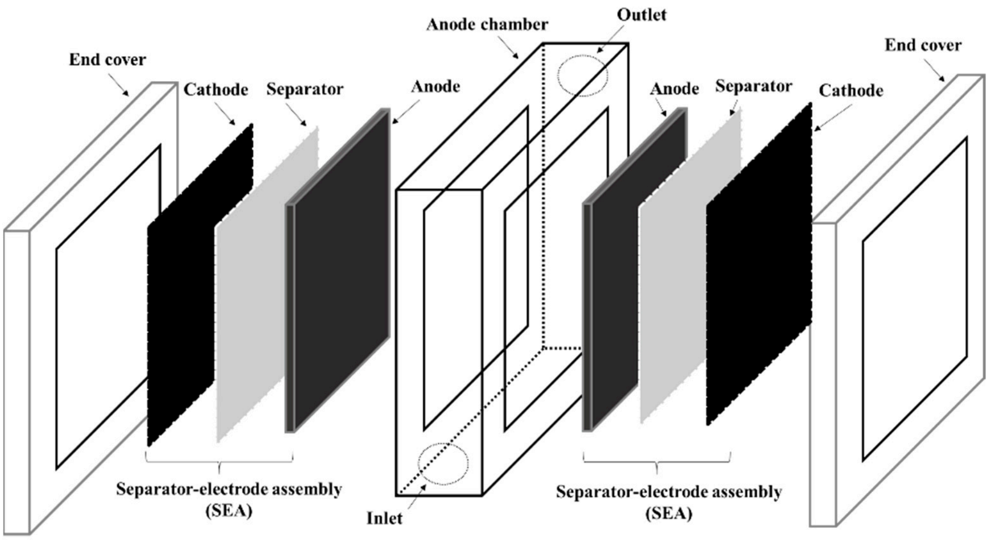

Figure 1. The schematic diagram of microbial fuel cell in this study.

2.2. Operating Conditions

All anode compartments were inoculated with activated return sludge (6000 mg-VSS/L) obtained from a municipal wastewater treatment plant (WWTP) (Busan, Korea). The sludge was circulated for 24 h. Subsequently, the three MFCs using synthetic WW were operated individually (phase I) for 40 days. And then the three MFC were connected hydraulically from S-MFC to L-MFC in series for 160 days; phase II for forward flow (ascending connection) and phase III for reverse flow (descending connection) (Figure 2). Power generation was also tested in phases II and III according to the electrode connection method (in series and parallel). All MFCs were operated at the same flow rate (38.4 mL/h) and room temperature (24 ± 7.5 °C). A synthetic WW contains glucose, 0.5 g/L (500 mg-COD/L); K_2HPO_4, 0.035 g/L; $NaHCO_3$, 0.6 g/L; NH_4Cl, 0.5 g/L; NaCl, 0.04 g/L; $MgSO_4{\cdot}7H_2O$, 0.01 g/L; KCl, 0.02 g/L; $CaCl_2{\cdot}2H_2O$, 0.001 g/L and yeast extract, 0.005 g/L.

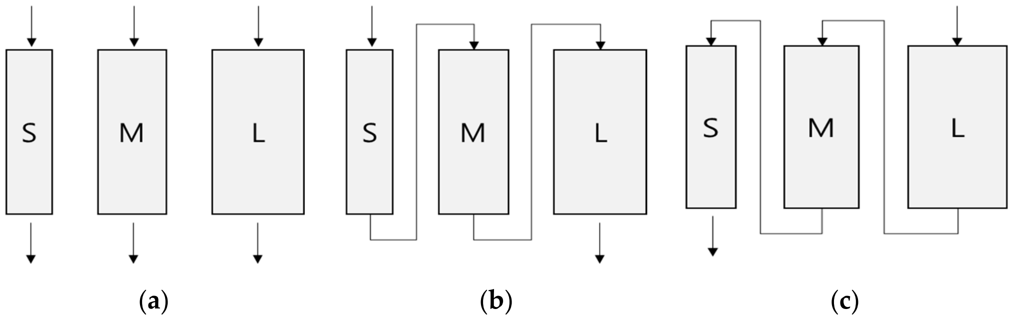

Figure 2. Diagram of a stacked microbial fuel cell (MFC) system operation according to the hydraulic flow connection mode: (**a**) Individual MFC operation (phase I), (**b**) a stacked MFC system operating in a forward hydraulic flow series connection mode (phase II), and (**c**) stacked MFC system operating in a reverse hydraulic flow series connection mode (phase III); the arrow means the direction of hydraulic flow.

2.3. Analyses and Calculations

The voltage (V) was acquired using a data acquisition system (Model 7700, Keithley Instruments Inc., Seoul, Korea) and recorded on a personal computer every 600 s. The polarization and power curves were acquired using linear sweep voltammetry (LSV) using a potentiostat (WMPG1000, WonATech Co., Seoul, Korea) at a scan rate of 0.1 mV/s. The polarization data used to acquire the MPD (W/m^2) were normalized by the total anode area, internal resistance, and open circuit voltage. The net energy recovery (ER) was calculated based on the previously reported equation [23]. The voltage loss was calculated using the following equation;

$$V_{loss}\ (\%) = ((V_{th} - V_{ac}))/V_{th} \times 100$$

where, V_{loss}, V_{th}, and V_a is the voltage loss, the theoretical voltage production of the stack system, and the actual voltage production, respectively.

Principal component analysis (PCA) and Pearson correlation coefficients were calculated using SPSS Statistics (Ver 25, IBM CO., New York, NY, USA). The soluble COD (SCOD) was measured with the colorimetric method of the US EPA using a CODCr test kit (HS-CODCr-M, Humas Co., Daejeon, Korea).

3. Results

3.1. Voltage Generation According to Hydraulic Flow Mode and Direction

Three MFCs (S-, M-, and L-MFCs) showed different voltage generations because of the different COD loading rates, removed CODs and other factors when all MFCs were operated individually (phase I) (Figures 3 and 4). L-MFC showed the highest voltage generation of 0.76 V, followed by M-MFC (0.52 V), and S-MFC (0.34 V) (Figure 4a). More substrate seemed to be used for electricity generation because of the highest COD loading rate of L-MFC. After a forward hydraulic series connection of three MFCs (phase II), it was expected that the amount of COD removed in three MFCs would become equal and the voltage of M- and L-MFCs decrease to the level of the voltage generated from S-MFC. On the other hand, the average voltage generation, COD loading rate, and removed COD of S- and M-MFCs did not changed much. While the average voltage generation of L-MFC decreased to 0.52 V, which appears to be caused by the decrease in COD removed (Figure 4b). M- and L-MFCs showed similar amounts of COD removed (187 mg/L and 204 mg/L, respectively), and produced the most similar voltage at phase II because of their similar the removed COD. On the other hand, all MFCs showed a different pattern of voltage generation under a reverse hydraulic series connection (phase III). Although M- and L-MFCs showed similar COD loading rates, they produced different voltages and the average voltage generation of L-MFC increased to 0.83 V because of its highest COD removal (Figure 4c). The voltage generation of S- and M-MFCs decreased to 0.14 V and 0.26 V, respectively.

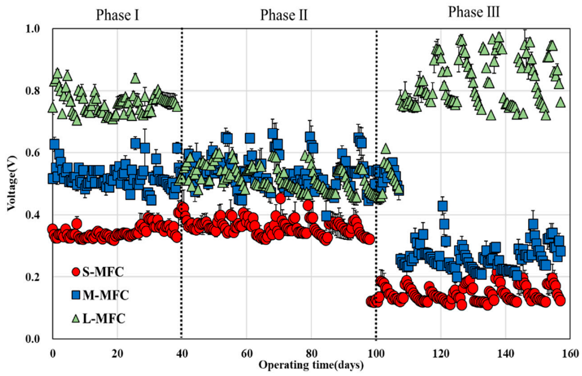

Figure 3. Voltage generation of S- (red circle), M- (blue square), and L-MFCs (green triangle) in a stacked MFC system according to the hydraulic flow connection mode and direction (phases I, II, and III).

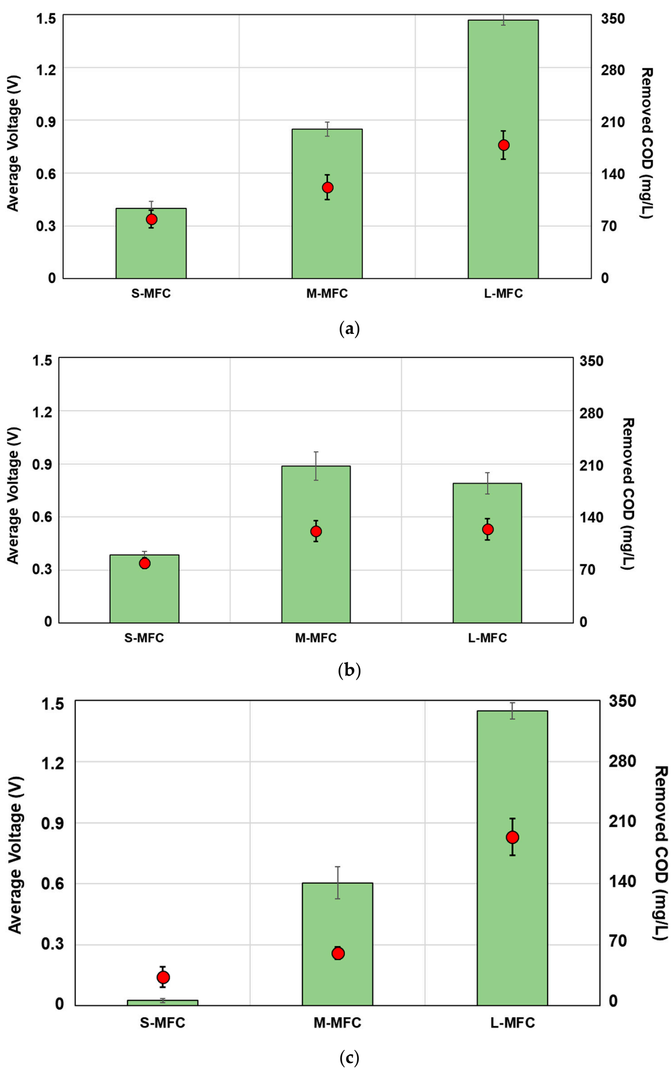

Figure 4. Removed chemical oxygen demand (COD) (green bar) and average voltage (red circle) of S-, M-, and L-MFCs at phase I (**a**), II (**b**), and III (**c**).

Electricity generation is generally affected by the organic loading rate, amount of COD removed, carbon source, reactors volumes, and other factors [24]. Two two-chamber MFCs produced similar cell voltage at different substrate concentrations and their stack systems were operated successfully without voltage reversal [25]. Single-chamber MFCs showed similar voltage generation at different organic loading rates because the bacterial activity, internal resistance, and reactor limitation could be different at each OLR [26]. In this study, despite the similar amounts of COD removed, M-MFC at phase III produced a lower voltage than its voltage at phases I and II because of various factors. The Pearson correlation showed that voltage generation was affected by several factors, including the reactor volume, HRT, influent COD concentration, loading rate, removed COD, and internal resistance (Table 2). In particular, voltage generation showed the highest Pearson correlation (0.9445) with the COD removed. In other words, the same the amount of COD removed can produce the same voltage because theoretically the same electrons and hydrogen ions can be generated from the same amount of COD removed. This indicates that equalizing the amount of COD removed can be a way to minimize the voltage imbalance between each MFC in a stack system.

Table 2. Pearson correlations of voltage and power density with the coulombic efficiency, energy recovery, reactor volume, hydraulic retention time (HRT), influent chemical oxygen demand (COD) concentration, influent COD loading rate, COD removal rate, removed COD concentration, the ratio of anode area for reactor volume, and internal resistance.

Parameter	Voltage	Power Density
Reactor volume	0.6385	0.3673
HRT	0.6385	0.3673
Influent COD concentration	0.6337	0.3008
Influent COD loading rate	−0.2373	−0.0640
COD removal rate	0.1168	0.1448
Removed COD	0.9445	0.3943
Internal resistance	−0.7460	−0.8313

3.2. Power Performances According to Hydraulic Flow Connection and Direction

All MFCs showed slightly different polarization and power curves according to the hydraulic flow connection and direction (Figure 5). Overall, S-MFC showed a lower MPD than M- and L-MFCs (Figure 5). This was attributed due to the rapid depletion of the substrate with decreasing HRT as the volume decreased under the same flow rate. In the case of MFC treated pharmaceutical sewage with different HRTs (8 and 5 h), short HRTs increased the volumetric organic loading rate, thereby reducing the MFC performance due to rapid substrate depletion [27].

Interestingly, some MFCs produced similar MPDs at each phase. The S- and L-MFCs showed similar MPDs (0.41–0.42 W/m^2) at phase I, and the M- and L-MFCs showed similar MPDs at phases II (0.61–0.64 W/m^2) and III (0.43–0.46 W/m^2) (Figure 5). In the case of a serial flow connection and direction, the carbon source type and COD removal rate would be different at each MFC because of the different reactor volumes, which can affect the power density. In general, glucose is converted to lactate, propionate, butyrate, and acetate [28]. The glucose-fed MFC showed a higher MPD of 1.5 W/m^2 than the acetate-fed (1.3 W/m^2), butyrate-fed (0.8 W/m^2), and propionate-fed (0.7 W/m^2) MFCs when using the same influent COD concentration [29]. Therefore, MFCs could produce the same power density due to a range of factors, including the COD concentrations, COD loading rate, and internal resistance [26,29]. In this study, the Pearson correlation showed that a range of factors influenced the power density, and there was a strong relationship with the internal resistance (Table 2). On the other hand, the MFCs do not produce the same MPD even if the MFCs produce the same voltage at the same external resistance.

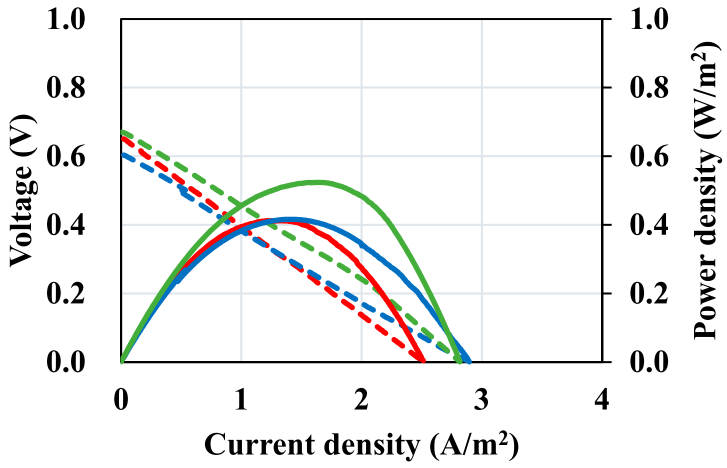

(**a**)

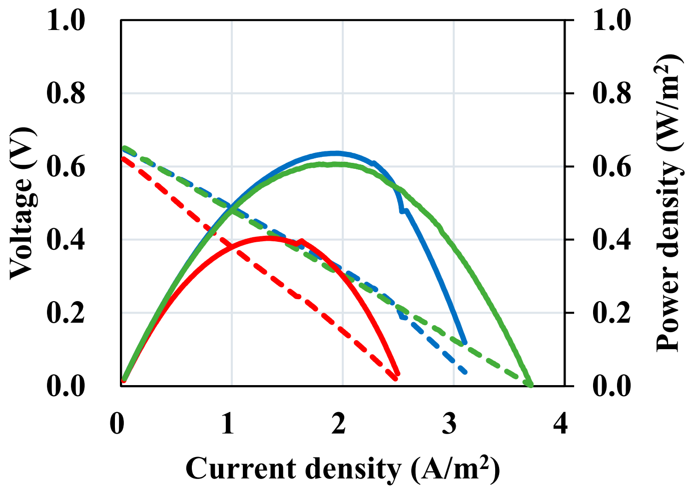

(**b**)

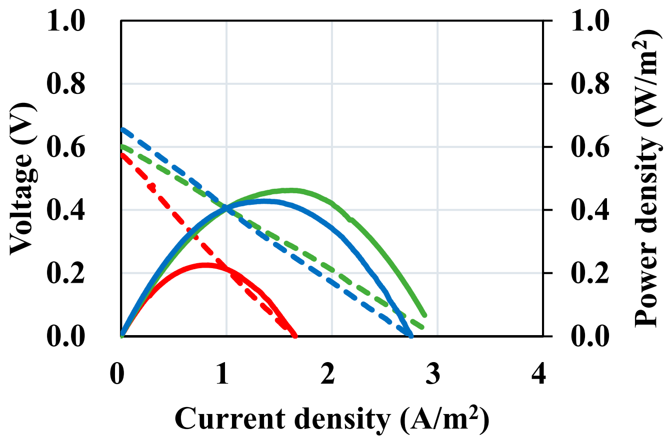

(**c**)

Figure 5. Polarization (dot line) and power curves (solid line) of S- (red), M- (blue), and L- (green) MFCs in a staked MFC system at phases I (**a**), II (**b**), and III (**c**).

3.3. Voltage Productions and Losses in Stacked Systems

The theoretical and actual voltage productions were compared according to the electrode connection method at each phase (Table 3). When the electrode was connected in series and parallel, the actual voltage production was lower than the theoretical voltage production regardless of the electrode connection method. In addition, voltage losses (28–74%) in a parallel electrode connection were lower than those (32–94%) in the electrode series connection, which is a similar trend in previous studies. The lower energy losses in a parallel connection generally occur because of the voltage reversal in the series connection and lower internal resistance in the parallel connection [18,30,31].

Table 3. Theoretical and actual measured voltage productions and voltage loss in a stacked system according to the electrode connection methods at phases I, II, and III.

Electrode connection	MFC Stacks [a]	Theoretical Voltage [b] (V)			Actual Voltage [c] (V)			Voltage Loss (%)		
		Phase I	Phase II	Phase III	Phase I	Phase II	Phase III	Phase I	Phase II	Phase III
Series	S-M	0.863	0.865	0.409	0.242	0.211	0.102	72.1	75.6	75.1
	S-L	1.103	0.844	0.975	0.116	0.264	0.095	89.5	68.7	90.3
	M-L	1.282	1.045	1.096	0.321	0.715	0.146	75.1	31.6	86.7
	S-M-L	1.624	1.377	1.240	0.101	0.143	0.094	93.8	89.6	92.4
Parallel	S-M	0.432	0.433	0.205	0.211	0.223	0.104	51.2	48.5	49.3
	S-L	0.552	0.422	0.488	0.312	0.209	0.101	43.5	50.5	79.3
	M-L	0.641	0.523	0.548	0.351	0.377	0.211	45.2	27.9	61.5
	S-M-L	0.541	0.459	0.413	0.212	0.221	0.109	60.8	51.9	73.6

[a] S-M; S- and M-MFCs stack, S-L; S- and L-MFCs stack, M-L; M- and L-MFCs stack, and S-M-L; S-, M-, and L-MFCs stack. [b] Theoretical voltage is calculated based on the actual voltage generated by the individual cells when individual cells are connected. [c] The actual voltage is actually measured voltage when the individual cells are connected.

Interestingly, the lowest voltage losses (28% for a parallel connection and 30% for a series connection) were observed when connected to M- and L-MFCs, producing similar voltage at phases II (M- and L-MFCs stack) (Figure 5). In contrast, the other stacks showed higher voltage losses (69–94% for series connection and 43–74% for parallel connection). This suggests that the simple hydraulically series connected stack system with different volume MFCs can minimize the voltage loss and avoid the voltage imbalance.

4. Conclusions

This study was the first attempt to minimize the voltage loss through a simple hydraulic connection of MFCs. The S-, M-, and L-MFCs showed different voltage productions at phase I (individual operation) because of a range of factors. When they were connected hydraulically in series (phase II), some MFCs produced a similar voltage by the same amount of COD removed. Moreover, the energy loss (<30%) could be minimized, even in the electric series and parallel connection. On the other hand, there was still high energy loss. Therefore, it will be necessary to find a solution through studies on the effects of the loading rates, actual wastewater, and long-term operations on the stack performance. This finding shows that connecting MFCs with different volumes can be a new option that can minimize the energy loss in an MFC stack system.

Funding: This study was supported financially by the National Research Foundation of Korea (NRF) grant funded by Korea Government (MIST) (No. 2015R1C1A1A01054204 and 2018R1D1A1B07046741) and by Korea Electric Power Corporation through Korea Electrical Engineering and Science Research Institute (No. R15XA03-01).

Institutional Review Board Statement: Not applicable.

Informed Consent Statement: Not applicable.

Data Availability Statement: The data presented in this study are available on request from the corresponding author.

Conflicts of Interest: The authors declare no conflict of interest and the funders had no role in the design of the study; in the collection, analyses, or interpretation of data; in the writing of the manuscript, or in the decision to publish the results.

References

1. An, J.; Sim, J.; Lee, H. Control of voltage reversal in serially stacked microbial fuel cells through manipulating current: Significance of critical current density. *J. Power Sources* **2015**, *283*, 19–23. [CrossRef]
2. An, J.; Kim, B.; Jang, J.K.; Lee, H.; Chang, I.S. New architecture for modulization of membraneless and single-chambered microbial fuel cell using a bipolar plate-electrode assembly (BEA). *Biosens. Bioelectron.* **2014**, *59*, 28–34. [CrossRef]
3. Andersen, S.J.; Pikaar, I.; Freguia, S.; Lovell, B.C.; Rabaey, K.; Rozendal, R.A. Dynamically adaptive control system for bioanodes in serially stacked bioelectrochemical systems. *Environ. Sci. Technol.* **2013**, *47*, 5488–5494. [CrossRef]
4. Chang, T.; Chang, Y.; Chao, W.; Jane, W.; Chang, Y. Effect of hydraulic retention time on electricity generation using a solid plain-graphite plate microbial fuel cell anoxic/oxic process for treating pharmaceutical sewage. *J. Environ. Sci. Health Part A* **2018**, *53*, 1185–1197. [CrossRef]
5. Cheng, S.; Liu, H.; Logan, B.E. Power densities using different cathode catalysts (Pt and CoTMPP) and polymer binders (Nafion and PTFE) in single chamber microbial fuel cells. *Environ. Sci. Technol.* **2006**, *40*, 364–369. [CrossRef]
6. Choi, J.; Ahn, Y. Continuous electricity generation in stacked air cathode microbial fuel cell treating domestic wastewater. *J. Environ. Manag.* **2013**, *130*, 146–152. [CrossRef]
7. Dekker, A.; Heijne, A.T.; Saakes, M.; Hamelers, H.V.; Buisman, C.J. Analysis and improvement of a scaled-up and stacked microbial fuel cell. *Environ. Sci. Technol.* **2009**, *43*, 9038–9042. [CrossRef]
8. Du, Z.; Li, H.; Gu, T. A state of the art review on microbial fuel cells: A promising technology for wastewater treatment and bioenergy. *Biotechnol. Adv.* **2007**, *25*, 464–482. [CrossRef]
9. Fischer, F.; Sugnaux, M.; Savy, C.; Hugenin, G. Microbial fuel cell stack power to lithium battery stack: Pilot concept for scale up. *Appl. Energy* **2018**, *230*, 1633–1644. [CrossRef]
10. Frank, M.; Kuhl, M.; Erdler, G.; Freund, I.; Manoli, Y.; Muller, C.; Reinecke, H. An integrated power supply system for low power 3.3 V electronics using on-chip polymer electrolyte membrane (PEM) fuel cells. *IEEE J. Solid State Circuits* **2010**, *45*, 205–213. [CrossRef]
11. Ge, Z.; Li, J.; Xiao, L.; Tong, Y.; He, Z. Recovery of Electrical Energy in Microbial Fuel Cells. *Environ. Sci. Technol. Lett.* **2014**, *1*, 137–141. [CrossRef]
12. Gurung, A.; Kim, J.; Jung, S.; Jeon, B.; Yang, J.E.; Oh, S. Effects of substrate concentrations on performance of serially connected microbial fuel cells (MFCs) operated in a continuous mode. *Biotechnol. Lett.* **2012**, *34*, 1833–1839. [CrossRef]
13. Juang, D.; Yang, P.; Chou, H.; Chiu, L. Effects of microbial species, organic loading and substrate degradation rate on the power generation capability of microbial fuel cells. *Biotechnol. Lett.* **2011**, *33*, 2147–2160. [CrossRef]
14. Khaled, F.; Ondel, O.; Allard, B.; Degrenne, N. Voltage balancing circuit for energy harvesting from a stack of serially-connected Microbial Fuel Cells. In Proceedings of the 2013 IEEE ECCE Asia Downunder, Melbourne, Australia, 3–6 June 2013; pp. 392–397.
15. Kim, D.; An, J.; Kim, B.; Jang, J.K.; Kim, B.H.; Chang, I.S. Scaling-Up Microbial Fuel Cells: Configuration and Potential Drop Phenomenon at Series Connection of Unit Cells in Shared Anolyte. *ChemSusChem* **2012**, *5*, 1086–1091. [CrossRef]
16. Kim, H.; Kim, B.; Yu, J. Power generation response to readily biodegradable COD in single-chamber microbial fuel cells. *Bioresour. Technol.* **2015**, *186*, 136–140. [CrossRef]
17. Kim, I.S.; Choi, M.J. Microbial fuel cells: Recent advances, bacterial communities and application beyond electricity generation. *Environ. Eng. Res.* **2008**, *13*, 51–65. [CrossRef]
18. Kim, Y.; Hatzell, M.C.; Hutchinson, A.J.; Logan, B.E. Capturing power at higher voltages from arrays of microbial fuel cells without voltage reversal. *Energy Environ. Sci.* **2011**, *4*, 4662–4667. [CrossRef]
19. Kim, H.; Kim, B.; Yu, J. Effect of HRT and external resistances on power generation of sidestream microbial fuel cell with CNT-coated SSM anode treating actual fermentation filtrate of municipal sludge. *Sci. Total Environ.* **2019**, *675*, 390–396. [CrossRef]
20. Logan, B.E.; Hamelers, B.; Rozendal, R.; Schröder, U.; Keller, J.; Freguia, S.; Aelterman, P.; Verstraete, W.; Rabaey, K. Microbial fuel cells: Methodology and technology. *Environ. Sci. Technol.* **2006**, *40*, 5181–5192. [CrossRef]
21. Nam, J.; Kim, H.; Lim, K.; Shin, H. Effects of organic loading rates on the continuous electricity generation from fermented wastewater using a single-chamber microbial fuel cell. *Bioresour. Technol.* **2010**, *101*, S33–S37. [CrossRef]
22. Park, Y.; Park, S.; Nguyen, V.K.; Yu, J.; Torres, C.I.; Rittmann, B.E.; Lee, T. Complete nitrogen removal by simultaneous nitrification and denitrification in flat-panel air-cathode microbial fuel cells treating domestic wastewater. *Chem. Eng. J.* **2017**, *316*, 673–679. [CrossRef]
23. Pham, T.H.; Aelterman, P.; Verstraete, W. Bioanode performance in bioelectrochemical systems: Recent improvements and prospects. *Trends Biotechnol.* **2009**, *27*, 168–178. [CrossRef]
24. Rahimnejad, M.; Ghoreyshi, A.; Najafpour, G.; Younesi, H.; Shakeri, M. A novel microbial fuel cell stack for continuous production of clean energy. *Int. J. Hydrogen Energy* **2012**, *37*, 5992–6000. [CrossRef]
25. Shimoyama, T.; Komukai, S.; Yamazawa, A.; Ueno, Y.; Logan, B.E.; Watanabe, K. Electricity generation from model organic wastewater in a cassette-electrode microbial fuel cell. *Appl. Microbiol. Biotechnol.* **2008**, *80*, 325–330. [CrossRef]
26. Wang, B.; Han, J. A single chamber stackable microbial fuel cell with air cathode. *Biotechnol. Lett.* **2009**, *31*, 387–393. [CrossRef]
27. Yazdi, H.; Alzate-Gaviria, L.; Ren, Z.J. Pluggable microbial fuel cell stacks for septic wastewater treatment and electricity production. *Bioresour. Technol.* **2015**, *180*, 258–263. [CrossRef]
28. Yu, J.; Park, Y.; Kim, B.; Lee, T. Power densities and microbial communities of brewery wastewater-fed microbial fuel cells according to the initial substrates. *Bioprocess Biosyst. Eng.* **2015**, *38*, 85–92. [CrossRef]

29. Yu, J.; Park, Y.; Cho, H.; Chun, J.; Seon, J.; Cho, S.; Lee, T. Variations of electron flux and microbial community in air-cathode microbial fuel cells fed with different substrates. *Water Sci. Technol.* **2012**, *66*, 748–753. [CrossRef]
30. Yu, J.; Seon, J.; Park, Y.; Cho, S.; Lee, T. Electricity generation and microbial community in a submerged-exchangeable microbial fuel cell system for low-strength domestic wastewater treatment. *Bioresour. Technol.* **2012**, *117*, 172–179. [CrossRef]
31. Zhuang, L.; Zheng, Y.; Zhou, S.; Yuan, Y.; Yuan, H.; Chen, Y. Scalable microbial fuel cell (MFC) stack for continuous real wastewater treatment. *Bioresour. Technol.* **2012**, *106*, 82–88. [CrossRef]